第 15卷 第 4期
2009年 11月
电化学
ELECTROCHEMISTRY
Vol 15 No. 4
Nov. 2009

Artical ID: 1006-3471 (2009) 04-0432-09

Enhanced Visible Light Photoelectrochemical Performances with Nitrogen Doped TiO_2 Nanowire Arrays

LV Xiao-jun[1], LI Yue-ming[1], ZHANG Hao[1], CHEN Da[1], Jennifer Hensel[2], Jin Z Zhang[2*], LI Jing-hong[1*]

(1. *Department of Chemistry, Tsinghua University, Beijing* 100084, *China*;
2. *Department of Chemistry and Biochemistry, University of California, Santa Cruz, California* 95064, *USA*)

Abstract: Self-organized anodic anatase TiO_2 nanowire arrays doped with nitrogen have been successfully fabricated and their photoelectrochemical (PEC) properties have been characterized and found to be substantially improved compared to undoped nanowires or commercial P25 nanoparticles. Photocurrent measured with monochromatic incident light showed that the incident photon-to-current efficiency (IPCE, %) values of nanowire array electrodes with or without N-doping were obviously higher than that of commercial P25 nanoparticle electrodes, and nitrogen-doped TiO_2 nanowire arrays (NTNA) had noticeable absorption in the visible region. The NTNA electrodes showed the highest photocurrent density and power conversion efficiency under 100 mW/cm^2 visible light illumination. A maximum photoconversion efficiency of 0.52% was achieved for the NTNA sample at an applied potential of 0.09 V versus Ag/AgCl (saturated KCl) electrode under visible illumination, much higher than that of the undoped nanowire and commercial P25 nanoparticle electrodes. These results demonstrate that NTNA thin films are promising for enhancing the photoresponse and effectively improving PEC performances of nanostructured TiO_2 in the visible region for different applications including solar hydrogen generation.

Key words: nitrogen doped; TiO_2 nanowire arrays; visible light; photoelectrochemical performances; photocatalysis

CLC Number: TB383 **Document Code:** A

TiO_2 as a wide bandgap n-type metal oxide semiconductor has been extensively investigated for water splitting due to its good stability, nontoxicity, low cost, and high catalytic activity [1-3]. Recently, there have been extensive studies on nanostructured TiO_2, such as noanotubes, nanowires and nanorods, as the electron transport materials due to their unique physical properties and wide range of applications [4-6]. Compared to nanoparticles, one dimensional (1D) nanostructures such as nanowires and nanorods have better charge transport properties while, in the meantime, they have larger surface area in comparison to bulk or two dimensional (2D) nanostructures. Thus, TiO_2 nanowires and nanorods are considered as highly desired structures for both photovoltaic and photoelectrochemical applications. Different strategies have

Received date: 2009-06-17, Accepted date: 2009-06-17
* Corresponding author, Tel: (86-10) 62795290, E-mail: jhli@mail.tsinghua.edu.cn
Supported by the National Natural Science Foundation of China (No. 20628303) and 863 Project (2006AA05Z123)

been developed for synthesizing TiO_2 nanowires and nanorods, including sol-gel [7], chemical vapor deposition (CVD) [8], solvothermal method [9], anodization[10] and glancing angle deposition (GLAD) [11]. Among these strategies, electrochemical anodization is relatively simple and provides a facile and direct approach for producing TiO_2 nanowires with high surface area and long wire length [10].

Despite the promising properties of TiO_2 nanowires mentioned above, the wide bandgap of TiO_2 (3.0 eV for rutile and 3.2 eV for anatase) limits its photoresponse mainly to the UV region, which accounts for only ~5% of solar spectrumolenergy. Much effort has been made to narrow the effective bandgap of TiO_2 while maintaining its superior charge transfer and transport properties and photocorrosion stability. It has been shown that nitroge-doping (N-doping) is an effective method to narrow the bandgap of anatase TiO_2 and thereby increase the visible light absorption [12-14]. For example, N-doping of TiO_2 nanotubes has been demonstrated using pure NH_3 [15]. TiO_2 nanowire arrays (TNA), especially when doped with N, are considered as promising for photoelectrochemical applications because of the combination of expected enhanced visible absorption and better charge transport along long nano wire. However, to date the study of TNA or N-doped TiO_2 nanowire arrays (NTNA) has been very limited.

In the present work, N-doped self-organized anodic TiO_2 nanowire arrays (NTNA) have been fabricated using a simple electrochemical approach. Optical and photoelectrochemical studies have shown that the NTNA electrodes had substantially enhanced visible light photoresponse and improved photoconversion efficiency compared to TNA and nanoparticle electrodes. These improved properties are expected to be useful in applications including solar energy conversion, water splitting for hydrogen generation, as well as photoelectrochemical degradation of pollutants.

1　Experimental Section

1.1　Preparation of TiO_2 Nanowire Arrays

TiO_2 nanowire arrays (TNA) were prepared by a modified method developed by Choi et al [10]. Typically, the polished Ti foil (0.25 mmolthick, 99.38% purity, fromol Beijing General Research Institute for Nonferrous Metals) was pretreated by rinsing in an ultrasonic bath of acetone, alcohol and deionized water for 5 min in turn, then chemically etched by immersing in a mixture solution of HF, HNO_3 and H_2O acids in the ratio of 1∶4∶5 (by Vol.) for 30 s, rinsed in an ultrasonic bath of acetone, isopropanol and methyl alcohol for 5 min in turn, and finally rinsed in deionized water. At the end, the obtained substrate was dried with N_2 at roomoltemperature.

The anodization process was carried out at roomoltemperature using a direct current power supply (Dahua Wireless Instrument Co., Beijing) in a two-electrode electrolytic cell, with the pretreated Ti foil serving as the anode and Pt foil serving as the cathode. The anodizing voltage increased gradually fromol 0 to 50 V with an increasing rate of 100 mV/s and was then kept at 50 V for 10 h. The electrolyte was 15 mL of ethylene glycol (EG) solution containing NH_4F (0.25%, by mass) and 500 μL deionized water. Generally, a small amount of water in the EG solution is essential for the formation of anodic TiO_2 nanowires at a high potential. After the anodization, the obtained substrate was immediately rinsed with deionized water and dried with a N_2 stream. Then, the anodized substrate was annealed at 450 ℃ in oxygen for 3 h with the cooling rate of 2 ℃ · min^{-1} to convert the amorphous phase to the anatase crystalline phase.

The process of introducing the nitrogen dopant was carried out in a tube furnace. The obtained TiO_2 nanowires were immersed in 0.5 mol · L^{-1} hexamethylenetetramine (HMT) solution for two days. Subsequently, the specimens were put in quartz tube, and the dopant was carried out by tube furnace at 400 ℃ for 1 h where N_2 acted as the carrier gas. After heating, the sample remained in the furnace until naturally cooling down to roomoltemperature.

1.2　Characterization

Powder X-ray diffraction (XRD) was performed on a Bruker D8-Advance X-ray powder diffractometer with monochromatized Kα radiation (λ = 0.15406 nm). The 2θ range used in the measurements was from 20° to 80°. X-ray photoelectron spectroscopy (XPS) studies of the films were carried out on an X-ray photoelectron spectrometer (PHI Quantera SXM) using a non-monochromatized Al Kα X-ray source (1486.6 eV). The energy resolution of the spectrometer was set at 0.5 eV, and the binding energy was calibrated using a C 1s (284.6 eV) spectrum of a hydrocarbon that remained in the XPS analysis chamber as a contaminant. SEM images were acquired on a field emission (FE) scanning electron microscope (JEOL JSM-7401F) operated at 3.0 kV. Mott-Schottky (MS) spectra were measured with a three-electrode cell, using the TiO_2-based samples as the working electrode, a platinum wire as the counter electrode, and a standard Ag/AgCl in saturated KCl as the reference electrode. The electrolyte was 0.1 mol·L^{-1} KNO_3 aqueous solution. Mott-Schottky (MS) spectra were obtained with a PARSTAT-2273 Advanced Electrochemical Systemol (Princeton Applied Research) controlled by a computer.

1.3 Photoelectrochemical Measurements

Photocurrent action spectra were measured in a two-electrode configuration, home-built experimental system, where the sintered TiO_2 photoanode served as the working electrode with an active area of about 1 cm^2 defined using Teflon tape and a platinum wire was used as the counter electrode. The generated photocurrent signal was collected by using a lock-in amplifier (Stanford Instrument SR830 DSP) synchronized with a light chopper (Stanford Instrument SR540). Photocurrent density vs bias potential characteristic was conducted with a three-electrode cell, using the sintered photoanode as the working electrode, a platinum wire as the counter electrode, and a standard Ag/AgCl in saturated KCl as the reference electrode. Photocurrent density vs bias potential characteristic spectra was obtained with a PARSTAT-2273 Advanced Electrochemical Systemol (Princeton Applied Research) controlled by a computer. A 500 W Xe lamp with a monochromator and equipped with AMOL 1.5 filter (filter off lights with wavelength shorter than 400 nm for 100 mW/cm^2 visible light measurements) respectively, was used as the light source. The electrolyte was 0.1 mol·L^{-1} KNO_3 aqueous solution. All measurements were carried out after bubbling N_2 for 20 min and controlled automatically by a computer.

2 Results and Discussion

2.1 Structural Properties of Nitrogen Doped TiO_2 Nanowire Arrays

Figure 1 shows typical FESEM images of the morphologies of TNA and NTNA. As shown in Figure 1a, the TiO_2 nanowires were more than 10 μm in length and 60 nm in diameter, and there remained the TiO_2 nanotubes with a diameter of about 100 nm underneath the nanowires. Figures 1b and c show different magnifications of TNA. Figure 1d shows that, after nitrogen doping, the morphologies of TNA did not obviously change, indicating that the N-doping process had little effect on the nanostructures of the as-prepared TNA. The morphologies of the TNA at low magnification were just like blooming flowers (Figures 1b and 1c), which seemed to follow the bamboo-splitting nanowire formation model[10], i.e., highly organized TiO_2 nanotubes firstly formed in Ti foil at the beginning of the anodization, and the nanotubes were then vertically split off into several parts by the electric-field-directed etching. The splitting led to the formation of NTNA on the entire TiO_2 nanotube arrays.

Figure 2 shows the XRD patterns of fabricated TNA, NTNA and Ti foil. According to the XRD results, the diffraction peaks of Ti foil could be indexed into hexagonal phase (ICDD-JCPDS No. 44-1294). The diffraction peaks of TNA shown in curve b in Figure 2 could be indexed into anatase phase (ICDD-JCPDS No. 21-1272). As shown in curve c in Figure 2, the peaks of N-doped TNA showed no obvious change compared with those of TNA, which means the N-doping process did not change the phase of TNA.

The N - bonding information and the effect of

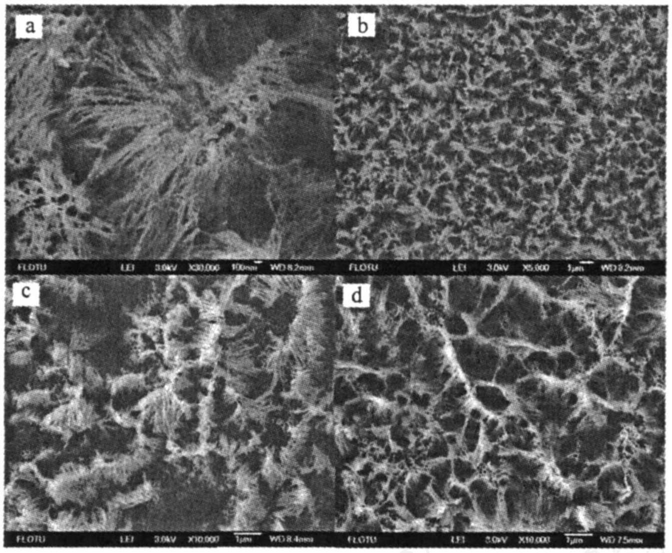

Fig 1 FE-SEM images of (a), (b) and (c) different magnified TiO_2 nanowire arrays, (d) N-doped TiO_2 nanowire arrays

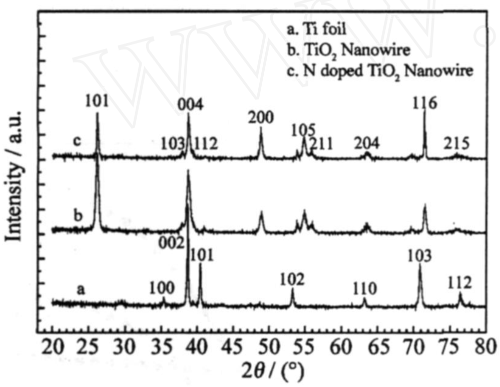

Fig 2 XRD patterns of (a) Ti foil, (b) TiO_2 nanowires and (c) N doped TiO_2 nanowires

nitrogen doping on the optical properties of NTNA were identified by the XPS technique. From Figure 3a, it can be seen that the NTNA contained Ti, O, N and C, and the binding energies of Ti 2p, O 1s, C 1s, and N 1s were 459.7 eV, 530.2 eV, 400.2 eV and 284.9 eV, respectively. Figure 3b shows the XPS spectra of only the nitrogen binding energies from 396 eV to 412 eV with three peaks at 398.7 eV, 400.2 eV and 405 eV, respectively. The XPS spectra of Ti $2p_{3/2}$ and O 1s peaks are shown in Figure 3c, which verified the substitution of N for O in TiO_2 crystals [16].

As Figure 3b shows, the peak at 400.2 eV corresponds to molecularly chemisorbed nitrogen (γ-N_2) at the surface [14, 17] or N atoms from N—N, N—H, O—N or N-containing organic compound absorbed on the surface [13]. It has been reported that the N 1s features appearing above 400 eV is due to Ti—O—N linkage [18], suggesting that some nitrogen atoms were doped in the interstitial sites of TNA lattices. In addition, the intense peak at 405.3 eV could be originated from nitrite ions [19], and the peak at 398.7 eV was assigned to nitrogen atoms which substituted for O and doped into the crystal lattices of nanowires to form the Ti-N bonds [20-21].

As for the Ti $2p_{3/2}$, a peak is located at 458.9 eV for NTNA (Figure 3c), which was significantly lower than that of P25 TiO_2 powders (459.7 eV) [22] and TiO_2 nanowires (459.3 eV) [17], also indicating the nitrogen incorporation into the TNA. And the Ti $2p_{1/2}$ at 463.5 eV peak was characteristic of the Ti^{IV} oxidation state [17]. The lower binding energy of Ti $2p_{3/2}$ in the NTNA showed that the electronic interaction of Ti with anions was significantly different from that of TiO_2 nanoparticles and nanowires, where the interaction was between Ti and O rather than N. It is known that the lower electron negativity of nitrogen compared with that of oxygen resulted in a decrease in percent ionicity and electron density around the N anion, causing the increase of the Ti electron density [22].

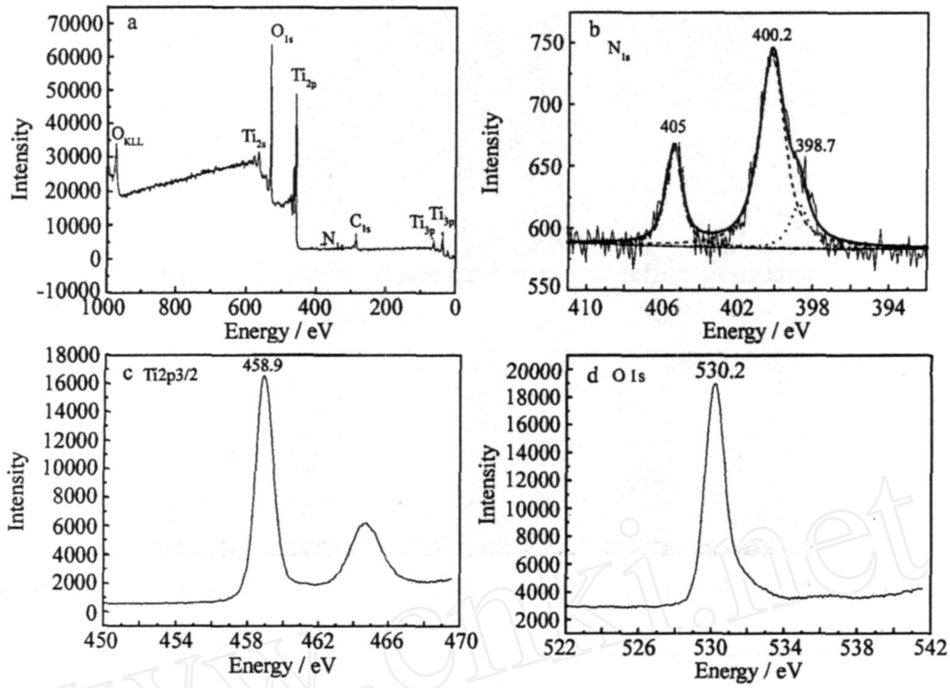

Fig 3 XPS spectra of N-doped TiO_2 nanowires a elemental survey, b N 1s, c Ti $2p_{3/2}$, d O 1s

The O 1s peak appeared at around 530.2 eV corresponding to Ti—O in Figure 3d, which was similar to that for the TiO_2 nanowires[17], indicating that there was no discernible change in the chemical environment for oxygen. In addition, broadening on the higher bonding energy band for N-TiO_2 at 531.4 eV could be found. The appearance of this additional peak was attributed to the nitridation process. This feature was previously assigned to the presence of another kind of oxygen in N-TiO_2[22]. On the basis of the above results and analysis, XPS results indicate that N doping into the crystal mainly results in Ti—N or N—Ti—O bonding.

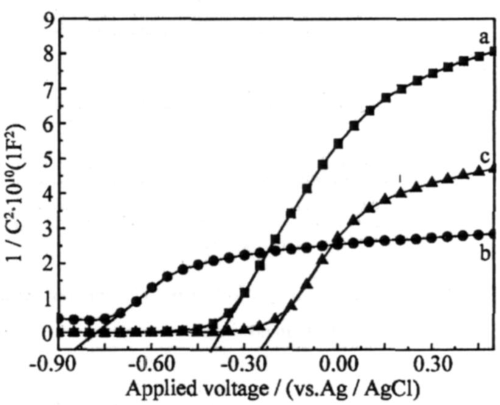

Fig 4 Mott-Schottky plots of for P25 nanoparticle films (a), TiO_2 nanowires (b) and N-doped nanowires (c) electrodes Mott-Schottky measurements were done at the frequency of 1 kHz in the aqueous solution of 0.1 mol $\cdot L^{-1}$ KNO_3, pH 7.5

2.2 Mott-Schottky (MS) Studies

Figure 4 shows Mott-Schottky (MS) measurement results, which were used to determine the difference in electronic properties of the TNA electrodes with or without N-doping[23-24]. As is clear from Figure 4, reversed sigmoidal plots were observed with an overall shape consistent with that typical for n-type semiconductors; And the reproducible flat-band potentials could be obtained from the intercepts of the linear region[25]. TNA electrodes showed a large positive shift of the conduction band as compared with the P25 nanoparticle electrodes, and NTNA had more positive flat-band potential than TNA electrodes.

It is well known that the presence of a large number of surface states can lead to a considerable change of the band position[26]. In most cases, a large number of surface states or oxygen vacancies are present in the P25 TiO_2 nanoparticles, whereas TiO_2

nanowire structures have a lower density of surface states or oxygen vacancies that can lead to a change of the band position. Furthermore, in the case of NTNA, N atoms could substitute for some oxygen vacancies and reduce the recombination centers of charge carriers, leading to the much higher photocurrent density observed in comparison to the P25 nanoparticles. Mott-Schottky results show that the NTNA electrodes have lower density of surface states and thereby improve charge transport properties, which are useful for enhancing photocurrent density.

2.3 Photoelectrochemical Characterization

Photocurrent measurements with monochromatic incident light of P25 TiO_2 nanoparticles and TNA with and without N-doping were performed without bias in a two-electrode configuration. The illumination area of the photoanode was about 0.12 cm^2. The incident photon-to-current efficiency (IPCE) was calculated using the following equation [3]:

$$\mathrm{IPCE}/\% = \frac{(1240\,\mathrm{eV}\cdot\mathrm{nm})\,(\text{photocurrent density}\ \mu\mathrm{A/cm^2})}{(\lambda\,\mathrm{nm})\,(\text{irradiance}\ \mu\mathrm{W/cm^2})} \times 100 \quad (1)$$

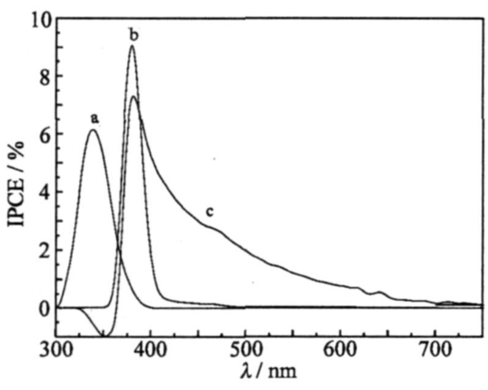

Fig 5 Incident photon-to-current efficiency (IPCE) spectra with monochromatic light at different wavelengths of P25 nanoparticles (a), TiO_2 nanowires (b) and N-doped TiO_2 nanowires (c) as photoanodes in 0.1 mol · L^{-1} KNO_3 solution under Xe lamp irradiation

As shown in Figure 5, the maximum IPCE (%) values of NTNA and TNA electrodes reached 7.2% and 9% at 380 nm, respectively, obviously higher than 4% measured for P25 TiO_2 thin film electrodes at 340 nm. The NTNA electrodes also showed noticeably higher photocurrent in the visible region, extending all the way to about 675 nm. In contrast, the undoped TNA and TiO_2 nanoparticles exhibited little or no photoresponse in the visible region. NTNA and TNA electrodes showed an apparent photocurrent maximumolat about 380 nm, while the P25 TiO_2 layer electrodes showed a photocurrent maximum at about 340 nm. The positions of the photocurrent maximum are likely related to bandgap as well as the effective light absorption and scattering of the nanostructure films. The bandgap of anatase TiO_2 is at 387 nm or 3.2 eV[14].

The higher IPCE (%) values of NTNA and TNA than P25 TiO_2 nanoparticle electrodes could be attributed to the different space charge layer within the wire wall[27]. Compared to random structures, the ordered nanowire array structures could also allow for reduced scattering and enhanced photoabsorption[28], similar to photonic crystals or gratings. In addition, the higher crystallinity of TiO_2 nanowires could also enable more efficient electron injection and transport within the array electrodes, leading to longer electron lifetime and diffusion length in TiO_2 nanowires compared to nanoparticles[29]. It is clear that N doping is an effective way to improve the visible absorption of anatase TiO_2 by decreasing the effective TiO_2 bandgap with N-TiO_2 as a result of either mixing O2p states with its 2p states[3] or creating isolated N2p states above the valence band maximumolof TiO_2[30-31]. And nitrogen doping into TiO_2 substituted oxygen and decreased the surface oxygen concentration in TiO_2 crystalline structure leading to lower maximum peak of IPCE of NTNA than that of TNA.

Figure 6 shows that the photocurrent density as a function of applied potentials for the NTNA, TNA and P25 electrodes in 0.1 mol · L^{-1} KNO_3 solution under 100 mW / cm^2 visible light irradiation. The dark current density was found to be negligible, and the photocurrent density of nanoparticle electrodes was very low in the visible. However, the photocurrent densities of the NTNA and TNA electrodes were much higher in the visible; and, furthermore, the photocurrent density of the NTNA electrodes was about three times as much as that of the TNA electrodes. Considering the results in Figure 4, this result is consistent with the expectation of enhanced photocurrent density for the NTNA electrodes.

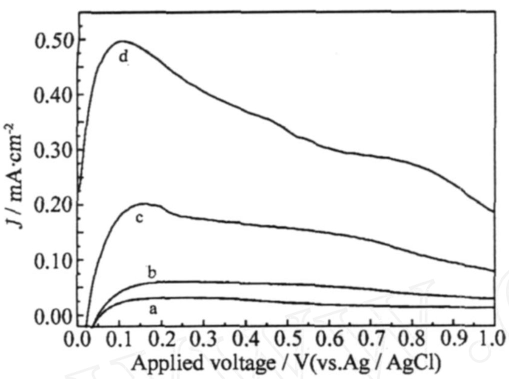

Fig 6　Variation of photocurrent density vs bias potential for P25 nanoparticle films (b), TiO_2 nanowires (c) and N-doped TiO_2 nanowires (d) in 0.1 mol·L^{-1} KNO_3 solution under visible light illumination

The photoconversion efficiency η of light energy to chemical energy in the presence of an external applied potential could be calculated according to the following equation[32]:

$$\eta(\%) = \frac{(\text{total power output} - \text{electrical power output})}{\text{light power input}} \times 100 = j_p \frac{(E^0_{rev} - |E_{app}|)}{I_0} \times 100 \quad (2)$$

where j_p is the photocurrent density (mA/cm^2), $j_p(E^0_{rev})$ is the total power output, $j_p|E_{app}|$ is the electrical power input, and I_0 is the power density of the incident light (mW/cm^2). E^0_{rev} is the standard reversible potential (which is 1.23 V for the water-splitting reaction), and $|E_{app}|$ is the absolute value of the applied potential E_{app}, which is obtained as

$$E_{app} = (E_{meas} - E_{ocp}) \quad (3)$$

where E_{meas} is the electrode potential of the working electrode at which j_p is measured under 100 mW/cm^2 visible light illumination, and E_{ocp} is the applied potential at open circuit under the same illumination at which j_p is measured in the same electrolyte solution. E_{meas} and E_{ocp} are with respect to the same Ag/AgCl (saturated KCl) reference electrode.

Figure 7 shows that the photoconversion efficiency as a function of applied potential for the different photoanodes studied. According to Eq. 2, a maximumol photoconversion efficiency of 0.52% was obtained for the NTNA electrodes at an applied potential of 0.09 V versus Ag/AgCl (saturated KCl) electrode under 100 mW/cm^2 visible light illumination. However, under the same condition, a maximum photoconversion efficiency of 0.2% was observed for the TNA electrodes at an applied potential of 0.15 V, and a maximum photoconversion efficiency of 0.05% was achieved for the P25 nanoparticles at an applied potential of 0.17 V. The results clearly indicate that the NTNA electrodes could harvest visible light more effectively than the TNA electrodes and P25 nanoparticle electrodes under the same irradiation. The efficiency for NTNA in the visible compares favorably well with obviously reported efficiency of 0.27% for TiO_2 nanotubes doped with boron[4].

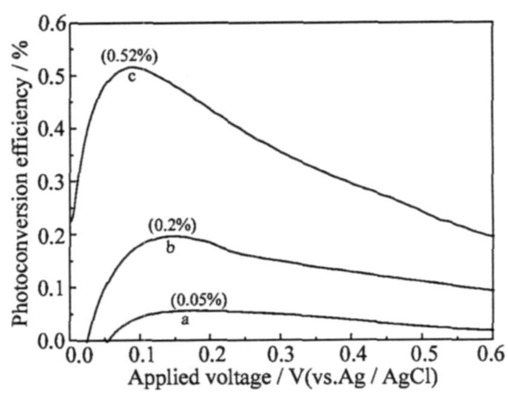

Fig 7　Photoconversion efficiency as a function of applied potential in 0.1 mol·L^{-1} KNO_3 solution for P25 nanoparticle (a), TiO_2 nanowire (b) and N-doped TiO_2 nanowire (c) electrodes under visible light illumination

3　Conclusions

In summary, self-organized anodic anatase TiO_2 nanowire arrays doped with nitrogen have been successfully fabricated and systematically investigated using a combination of FESEM, XRD, XPS, Mott-Schottky and photoelectrochemistry techniques. The structure of NTNA has been found to be in anatase phase. Nitrogen doping into the TiO_2 lattice results in a red-shift of absorption and enhanced photocurrent response in visible region relative to undoped TiO_2 films. Photocurrent measured with monochromatic incident light showed the IPCE (%) values of NTNA electrodes were obviously higher than that of commercial P25 nanoparticle electrodes. Furthermore, NTNA electrodes displayed a clear increase in its saturated photocurrent density under 100 mW/cm^2 visible light illumination than the undoped electrodes. A maximum photoconversion efficiency of 0.52% for NTNA electrodes was obtained, which was much higher than that on TNA and commercial P25 nanoparticle electrodes. The results suggest that N-doped TiO_2 nanowire arrays have good prospect for solar energy and other applications due to their improved optical and photoelectrochemical performances.

References:

[1] Fujishima A, Honda M. Electrochemical photolysis of water at a semiconductor electrode[J]. Nature, 1972, 238: 37.

[2] Han W Q, Wu L J, Klie R F, et al. Enhanced optical absorption induced by dense nanocavities inside titania nanorods[J]. Adv Mater, 2007, 19: 2525.

[3] Mor G K, Prakasamol H E, Varghese O K, et al. Vertically oriented Ti-Fe-O nanotube array films: toward a useful material architecture for solar spectrumolwater photoelectrolysis[J]. Nano Lett, 2007, 7: 2356.

[4] Lu N, Quan X, Li J Y, et al. Facile method for fabricating boron-doped TiO_2 nanotube array with enhanced photoelectrocatalytic properties[J]. J Phys Chem C, 2007, 111: 11836.

[5] Zhou J, Ding Y, Deng S Z, et al. Three-dimensional tungsten oxide nanowire networks[J]. Adv Mater, 2005, 17: 2107.

[6] Kimol D, Ghicov A, Albu S P, et al. Bamboo-type TiO_2 nanotubes: improved conversion efficiency in dye-Sensitized solar cells[J]. J Am Chem Soc, 2008, 130: 16454.

[7] Boercker J E, Enache-Pommer E, Aydil E S. Growth mechanismolof titanium dioxide nanowires for dye-sensitized solar cells[J]. Nanotechnology, 2008, 19: 095604.

[8] Lee J C, Sung Y M, KimolT G, et al. TiO_2-CdSe nanowire arrays showing visible-range light absorption[J]. Appl Phys Lett, 2007, 91: 113104.

[9] Wang G, Wang Q, Lu W, et al. Photoelectrochemical study on charge transfer properties of TiO_2-B nanowires with an application as humidity sensors[J]. J Phys Chem B, 2006, 110: 22029.

[10] Lim J H, Choi J. Titanium oxide nanowires originating from anodically grown nanotubes[J]. Small, 2007, 3: 1504.

[11] Wolcott A, Smith W A, Kuykendall T R, et al. Photoelectrochemical water splitting using dense and aligned TiO_2 nanorod arrays[J]. Small, 2009, 5: 104.

[12] Yu A, Wu G J, Zhang F X, et al. Synthesis and characterization of N-doped TiO_2 nanowires with visible light response[J]. Catal Lett, 2009, 129, 507.

[13] López-Luke T, Wolcott A, Xu L P, et al. Nitrogen-doped and CdSe quantum-dot-sensitized nanocrystalline TiO_2 films for solar energy conversion applications[J]. J Phys Chem C, 2008, 112: 1282.

[14] Asahi R, Morikawa T, Ohwaki T, at al. Visible-light photocatalysis in nitrogen-doped titanium oxides[J]. Science, 2001, 293: 269.

[15] Vitiello R P, Macak J M, Ghicov A, et al. N-doping of anodic TiO_2 nanotubes using heat treatment in ammonia[J]. Electrochem Commun, 2006, 8: 544.

[16] Chen X B, Lou Y, Samia A C S, et al. Formation of oxynitride as the photocatalytic enhancing site n nitrogen-doped titania nanocatalysts: comparison to a commercial nanopowder[J]. Adv Funct Mater, 2005, 15: 41.

[17] Martínez-Ferrero E, Sakatani Y, Boissière C, et al. Nanostructured titanium oxynitride porous thin films as efficient visible-active photocatalysts[J]. Adv Funct Mater, 2007, 17: 3348.

[18] Moribe S, Ikoma T, Akiyama K, et al. Photoinduced excited state proton rearrangement of 6-hydroxyquinoline along a hydrogen-bonded acetic acid wire[J]. Chem Phys Lett, 2007, 436: 373.

[19] Navio J A, Cerrillos C C, Real C. Photo-induced transformation, upon UV Illumination in air, of hyponitrite species $N_2O_2^{2-}$ preadsorbed on TiO_2 surface[J]. Surf Interface Anal, 1996, 24: 355.

[20] Chen S Z, Zhang P Y, Zhang D M. Investigation of nitrogen doped TiO_2 photocatalytic films prepared by

reactive magnetron sputtering [J]. Catal Commu, 2004, 11: 677.

[21] Wu P G, Ma C H, Shang J K. Effects of nitrogen doping on optical properties of TiO_2 thin films[J]. Appl Phys A, 2005, 81: 1411.

[22] Song X, Gao L. Synthesis, characterization, and optical properties of well-defined N-doped, hollow silica/titania hybrid microspheres[J]. Langmuir, 2007, 23: 11850.

[23] Chen D, Gao Y F, Wang G, et al. Surface tailoring for controlled photoelectrochemical properties: effect of patterned TiO_2 microarrays [J]. J Phys Chem C, 2007, 111: 13163.

[24] Fabregat-Santiago F, Garcia-Belmonte G, Bisquert J, et al. Mott-Schottky analysis of nanoporous semiconductor electrodes in the dielectric state deposited on SnO_2 conducting substrates [J]. J Electrochem Soc, 2003, 150: E293.

[25] Wang G, Lu W, Li J H, et al. V-shaped tin oxide nanostructure featuring broad photocurrent spectra: an effective visible-light driven photocatalyst[J]. Small, 2006, 12: 1436.

[26] Hagfeldt A, Bjorksten U, Gratzel M. Photocapacitance of nanocrystalline oxide semiconductor films: band-edge movement in mesoporous TiO_2 electrodes during UV illumination[J]. J Phys Chem, 1996, 100: 8045.

[27] Beranek R, Tsuchiya H, Sugishima T, et al. Enhancement and limits of the photoelectrochemical response from anodic TiO_2 nanotubes [J]. Appl Phys Lett, 2005, 87: 243114.

[28] Ong K G, Varghese O K, Mor G K, et al. Water-photolysis properties of micron-length highly-ordered titania nanotube-arrays [J]. J Nanosci Nanotechnol, 2005, 5: 1801.

[29] Ohsaki Y, Masaki N, Kitamura T, et al. Dye-sensitized TiO_2 nanotube solar cells: fabrication and electronic characterization [J]. Phys Chem Chem Phys, 2005, 7: 4157.

[30] Lee J Y, Park J, Cho J H. Electronic properties of N- and C-doped TiO_2 [J]. Appl Phys Lett, 2005, 87: 011904.

[31] Long M, Cai W, Wang Z, et al. Correlation of electronic structures and crystal structures with photocatalytic properties of undoped, N-doped and I-doped TiO_2 [J]. Chem Phys Lett, 2006, 420: 71.

[32] Khan S U M, Al-Shahry M, Ingler W B Jr. Efficient photochemical water splitting by a chemically modified n-TiO_2 [J]. Science, 2002, 297: 2243.

氮掺杂 TiO_2 纳米线阵列优越的可见光光电性能

吕小军[1], 李悦明[1], 张 昊[1], 陈 达[1], Jennifer Hensel[2], 张金中[2*], 李景虹[1*]

(1. 清华大学化学系,北京 100084; 2. 美国加利福尼亚大学 Santa Cruz分校化学与生物化学系, 美国 加利福尼亚)

摘要: 成功制备了氮掺杂锐钛矿 TiO_2 纳米线,并研究了它的光电化学性质. 结果表明,与商用 P25 TiO_2 纳米粒子和未掺杂 TiO_2 纳米线相比,氮掺杂 TiO_2 纳米线作为光阳极明显地提高了光电转换效率(IPCE%),在可见光区有明显光吸收;在 100 mW/cm^2 可见光光照下,氮掺杂 TiO_2 纳米线具有最大的光电流密度和能量转换效率. 例如,当电压为 0.09 V (vs Ag/AgCl)时最大能量转换效率为 0.52%,均高于未掺杂 TiO_2 纳米线和商用 P25 TiO_2 纳米粒子的,充分表现出它优越的光响应和光电化学性能,在光电化学池、太阳能制氢等方面具有广泛的应用前景.

关键词: 氮掺杂; TiO_2 纳米线阵列; 可见光吸收; 光电化学; 光催化